# Fluoride Effects along the Reaction Pathway of Pyrophosphatase: Evidence for a Second Enzyme·Pyrophosphate Intermediate†

Alexander A. Baykov,*,‡ Igor P. Fabrichniy,‡ Pekka Pohjanjoki,§ Anton B. Zyryanov,‡ and Reijo Lahti*,§

*A. N. Belozersky Institute of Physico-Chemical Biology and School of Chemistry, Moscow State University, Moscow 119899, Russia, and Department of Biochemistry, University of Turku, FIN-20014 Turku, Finland*

*Received March 17, 2000; Revised Manuscript Received June 22, 2000*

ABSTRACT: The fluoride ion is a potent and specific inhibitor of cytoplasmic pyrophosphatase (PPase). Fluoride action on yeast PPase during $PP_i$ hydrolysis involves rapid and slow phases, the latter being only slowly reversible [Smirnova, I. N., and Baykov, A. A. (1983) *Biokhimiya 48*, 1643−1653]. A similar behavior is observed during yeast PPase catalyzed $PP_i$ synthesis. The amount of enzyme·$PP_i$ complex formed from solution $P_i$ exhibits a rapid drop upon addition of fluoride, followed, at pH 7.2, by a slow increase to nearly 100% of the total enzyme. The slow reaction results in enzyme inactivation, which is not immediately reversed by dilution. These data show that fluoride binds to an enzyme·$PP_i$ intermediate during the slow phase and to an enzyme·$P_i$ intermediate during the rapid phase of the inhibition. In *Escherichia coli* PPase, the enzyme·$PP_i$ intermediate binds $F^-$ rapidly, explaining the lack of time dependence in the inhibition of this enzyme. The enzyme·$PP_i$ intermediate formed during $PP_i$ hydrolysis binds fluoride much faster (yeast PPase) or tighter (*E. coli* PPase) than the similar complex existing at equilibrium with $P_i$. It is concluded that PPase catalysis involves two enzyme·$PP_i$ intermediates, of which only one (immediately following $PP_i$ addition and predominating at acidic pH) can bind fluoride. Simulation experiments have indicated that interconversion of the enzyme·$PP_i$ intermediates is a partially rate-limiting step in the direction of hydrolysis and an exclusively rate-limiting step in the direction of synthesis.

The enzymes that catalyze reversible phosphoryl transfer from polyphosphates to water are fundamental to cell energetics, yet their mechanisms of action remain poorly understood. This enzyme group includes inorganic pyrophosphatase (EC 3.6.1.1; PPase),[1] which hydrolyzes pyrophosphate ($PP_i$) to orthophosphate ($P_i$), providing a thermodynamic pull for biosynthetic reactions (*1*). The two best studied PPases are those from *Saccharomyces cerevisiae* (Y-PPase) and *Escherichia coli* (E-PPase) (*2*, *3*). Both of these enzymes require divalent metal ions for catalysis, with $Mg^{2+}$ conferring the highest activity (*4*), and are active with either three or four magnesium ions per active site (*5*−*7*).

The currently accepted kinetic scheme of PPase catalysis involves substrate ($MgPP_i$ or $Mg_2PP_i$) binding to a preformed enzyme·$Mg^{2+}$ complex, P−O bond breakdown by direct attack of water (*8*), and stepwise dissociation of two phosphate molecules (Scheme 1). All the steps shown in Scheme 1 are readily reversible, allowing formation of appreciable amounts of enzyme-bound $PP_i$ ($EM_{n+2}PP_i$) from enzyme and $P_i$ and explaining the rapid exchange of oxygen between [$^{18}$O]$P_i$ and [$^{16}$O]water catalyzed by PPase (*9*).

Scheme 1: $PP_i$−$P_i$ Equilibration by PPase[a]

$$EM_2 \rightleftharpoons EM_{n+2}PP \rightleftharpoons EM_{n+2}P_2 \rightleftharpoons EM_{n+1}P \rightleftharpoons EM_2$$

[a] E= enzyme, M = Mg, PP = $PP_i$, P = $P_i$, $n$ = 1 or 2.

PPase is one of a few enzymes inhibited at micromolar fluoride concentrations (*10*−*12*). The action of fluoride on Y-PPase (*13*), rat liver PPase (*14*), and the D67N variant of *E. coli* PPase (*15*) is biphasic: an instant (half-time <1 s) decrease in activity upon addition of fluoride to functioning enzyme is followed by a slower decline in the remaining activity on a time-scale of seconds or minutes, depending on inhibitor concentration. Fluoride is thus simultaneously a rapidly reversible and a tight, slowly binding inhibitor, according to the nomenclature of Morrisson and Walsh (*16*). In the slow phase, one $PP_i$ molecule, two $Mg^{2+}$ ions, and one $F^-$ ion become trapped in PPase (*17*). This inactive complex, which can be isolated by gel filtration, decays, regenerating active enzyme with a half-time of ∼1 h at 25 °C (*18*). Although fluoride can bind to Y-PPase in the absence of substrate, such binding is characterized by only moderate affinity ($K_d \approx 3$ mM) and is rapidly reversible (*13*). Fluoride and $PP_i$ thus mutually stimulate their binding to PPase. Interestingly, *E. coli* PPase is also strongly inhibited by $F^-$, but the inhibition is of a rapidly reversible type (*19*, *20*). It was initially suggested that $PP_i$ becomes covalently bound to enzyme in the $F^-$-stabilized complex (*18*), but later studies did not support this contention. The mechanism of PPase inhibition by fluoride remains to be determined.

Earlier studies of fluoride interaction with PPase have focused on the hydrolysis reaction. Here we investigate fluoride effects on the reverse $PP_i$ synthesis reaction, as well

† This work was supported by the Russian Foundation for Basic Research (Grants 97-04-48487, 00-04-48310, and 00-15-97907) and the Academy of Finland (Grants 35736 and 47513).

* To whom correspondence should be addressed. A.A.B.: tel 095-939-5541, fax 095-939-3181, e-mail baykov@genebee.msu.su; R.L.: tel 358-02-3336845, fax 358-02-3336860, e-mail reijo.lahti@utu.fi.

‡ Moscow State University.

§ University of Turku.

[1] Abbreviations: E-PPase, *Escherichia coli* PPase; PPase, inorganic pyrophosphatase; $P_i$, phosphate; $PP_i$, pyrophosphate; Y-PPase, yeast (*Saccharomyces cerevisiae*) PPase.

10.1021/bi000627u CCC: $19.00 
Published on Web 09/02/2000

as on the enzyme·$PP_i$ intermediate in both reactions. The results of these studies indicate the occurrence of two types of enzyme·$PP_i$ intermediate in PPase catalysis and also show that the fast and slow phases of fluoride binding to Y-PPase designate different reaction intermediates in Scheme 1.

## EXPERIMENTAL PROCEDURES

*Enzymes.* Expression and purification of Y-PPase was carried out as described by Heikinheimo et al. (*21*), using the overproducing *E. coli* XL2blue[b] strain transformed with a vector including the coding region of yeast *PPA* gene under the *tac* promoter. Enzyme concentration was calculated on the basis of the subunit molecular mass of 32 kDa (*22*) considering $A^{1\%}_{280}$ equal to 14.5 (*4*), or by the Bradford assay (*23*). Wild-type E-PPase was obtained as described by Salminen et al. (*24*) and quantified using $A^{1\%}_{280}$ equal to 11.8 (*25*). Stock enzyme solutions were made in 0.1 M Tris/HCl buffer (pH 7.2) containing 1 mM $MgCl_2$ and 50 $\mu$M EGTA.

*Methods.* $PP_i$ hydrolysis was assayed by continuously recording $P_i$ liberation with an automatic $P_i$ analyzer (*26*). For use in the inhibition studies, the inlet system of the analyzer was modified to decrease its dead-time to 1 s as described previously (*13*, *14*). Measurements were carried out at constant concentrations of the substrate $Mg_2PP_i$ (0.2 mM) and free $Mg^{2+}$ (5 mM). Enzyme concentration was adjusted in order to get comparable absorbance values at different inhibitor concentrations.

$PP_i$ synthesis was assayed continuously by an enzyme-coupled procedure (*27*), using ATP-sulfurylase to convert the synthesized $PP_i$ into ATP, and using luciferase to monitor ATP formation. The assay mixture contained 20 mM potassium phosphate, 5 mM free $Mg^{2+}$, 5 $\mu$L of luciferin/luciferase solution (Sigma ATP assay mix, catalog no. FL-ASC, reconstituted with 5 mL of water), 0.7 unit/mL ATP-sulfurylase (Sigma), 10 $\mu$M adenosine 5′-phosphosulfate, 1 mM dithiothreitol, 1 mg/mL bovine serum albumin, and buffer in a total volume of 0.2 mL. The reaction was initiated by adding PPase, and the time-course of luminescence was followed with an LKB model 1250 luminometer. Care was taken to ensure that the ATP-sulfurylase concentration was sufficiently high, so that $PP_i$ conversion into ATP proceeded at least 20 times faster than $PP_i$ formation. The luminescence versus time curves measured in the absence of fluoride were slightly curved because of slow inactivation of luciferase in the reaction medium. The procedure used to measure enzyme-bound $PP_i$ formation at equilibrium was described previously (*28*).

$MgF^+$ formation ($K_d$ = 48 mM; *29*) was taken into account when calculating total $MgCl_2$ and free $F^-$ concentrations in the assays. To avoid $MgF_2$ formation and precipitation in the reaction mixture, fluoride was added just before the reaction was started with PPase. Sodium fluoride (Ultra grade) was purchased from Sigma Chemical Co.

Except as noted, the following pH buffers were used (0.1 M ionic strength, 50 mM $K^+$): 95 mM acetic acid/KOH, 100 $\mu$M EGTA (pH 4.8); 63 mM MES/KOH, 37 mM KCl, 100 $\mu$M EGTA (pH 5.5); 40 mM PIPES/KOH, 100 $\mu$M EGTA (pH 6.3); 83 mM TES/KOH, 17 mM KCl, 50 $\mu$M EGTA (pH 7.2); 90 mM TAPS/KOH, 5 $\mu$M EGTA (pH 8.5). The media used in the incubations with $P_i$ (synthesis of free and enzyme-bound $PP_i$) were prepared by mixing appropriate volumes of 100 mM potassium phosphate, 100 mM $MgCl_2$, and the buffers mentioned above, except that 20 mM acetic acid/KOH buffer was used at pH 4.8 and appropriate volumes of 1 M KOH were added to neutralize protons released upon $Mg^{2+}$·acetate complex formation. All experiments were performed at 25 °C.

Scheme 2: PPase Inactivation by Fluoride in the Course of $PP_i$ Hydrolysis

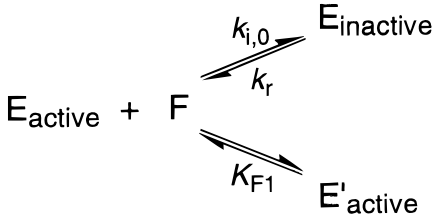


*Data Analysis and Calculations.* The time course of Y-PPase inactivation during enzymatic reaction is described by Scheme 2, which implies two modes of fluoride binding—rapid (not resolved in time) binding, leading to partially active enzyme ($E'_{active}$), and slow binding, leading to completely inactive enzyme ($E_{inactive}$). F is fluoride, $K_{F1}$ is the dissociation constant governing the rapid binding step, and $k_{i,0}$ and $k_r$ are the forward second-order and the backward first-order rate constants governing the slow binding step, respectively.

At zero time, only $E_{active}$ and $E'_{active}$ are present. The initial velocity of $PP_i$ hydrolysis in the presence of fluoride is given by eq 1, where $v_0$ and $v'_0$ are initial velocities at zero and infinite fluoride concentration, i.e., under conditions when all the enzyme is present as $E_{active}$ or $E'_{active}$, respectively, and $n = 1$. The apparent rate constant for slow fluoride binding, defined as $k_{i,app} = k_{i,0}[E_{active}]/([E_{active}] + [E'_{active}])$, is given by eq 2 with $n = 1$. The time-course of $P_i$ formation at fixed fluoride concentration is given by eqs 3 and 4, where $\alpha$ is the relative residual activity ($\alpha = \{[E_{active}] + v'_0[E'_{active}]/v_0\}/[E]_t$). For fitting of eqs 3 and 4, each product formation curve was represented by 90−200 pairs of [P] and $t$ values. The calculated and measured curves agreed within 3%. All fittings were carried out with the program SCIENTIST (MicroMath).

$$v_{0,app} = v'_0 + \frac{v_0 - v'_0}{1 + [F]^n/K_{F1}} \quad (1)$$

$$k_{i,app} = \frac{k_{i,0}}{1 + [F]^n/K_{F1}} \quad (2)$$

$$\frac{d[P]}{dt} = v_{0,app}\alpha \quad (3)$$

$$\frac{d\alpha}{dt} = k_r(1 - \alpha) - k_{i,app}[F]\alpha \quad (4)$$

## RESULTS

*Inhibition of Y-PPase-Catalyzed $PP_i$ Hydrolysis and Synthesis.* Figure 1 compares the effects of fluoride on the product formation curves in the two directions of the $PP_i \rightleftharpoons 2P_i$ equilibration by Y-PPase. In both directions, fluoride markedly decreased the initial velocity, with the effect on $PP_i$ synthesis being larger than on $PP_i$ hydrolysis at equal

Table 1: Parameters for Fluoride Inhibition of Y-PPase[a]

| source | substrate[b] | pH | $k_{i,0}$ ($mM^{-1}\cdot min^{-1}$) | $k_r$ ($min^{-1}$) | $K_{F1}$[c] | $K_{F2}$ (mM)[d] | $v_0'/v_0$ |
|---|---|---|---|---|---|---|---|
| inhibition of $PP_i$ hydrolysis | $PP_i$ (0.32) | 7.2 | $2.7 \pm 0.3$ | $\leq 0.03$ | $2.3 \pm 0.2$ | $\leq 0.011$ | $0.05 \pm 0.01$ |
| | | 8.5 | $0.94 \pm 0.03$ | $\leq 0.03$ | $6.4 \pm 0.2$ | $\leq 0.032$ | $\leq 0.02$ |
| inhibition of $PP_i$ synthesis | $P_i$ (20) | 7.2 | | | $1.6 \pm 0.2$ | | |
| inactivation in equilibrated | $P_i$ (20) | 7.2 | $0.21 \pm 0.02$ | $0.012 \pm 0.002$ | $0.65 \pm 0.07$ | 0.058 | |
| $PP_i \rightleftharpoons 2P_i$ system | $P_i$ (2) | 7.2 | $0.023 \pm 0.004$ | 0.012[e] | $0.9 \pm 0.3$ | | |

[a] Measured at 5 mM free $Mg^{2+}$. [b] Value in parentheses refers to total substrate concentration in millimoles per liter. [c] The units for $K_{F1}$ are mM (inhibition of $PP_i$ hydrolysis) or $mM^2$ (in all other cases). [d] $K_{F2} = k_r/k_{i,o}$. [e] Constrained at this value in the calculations.

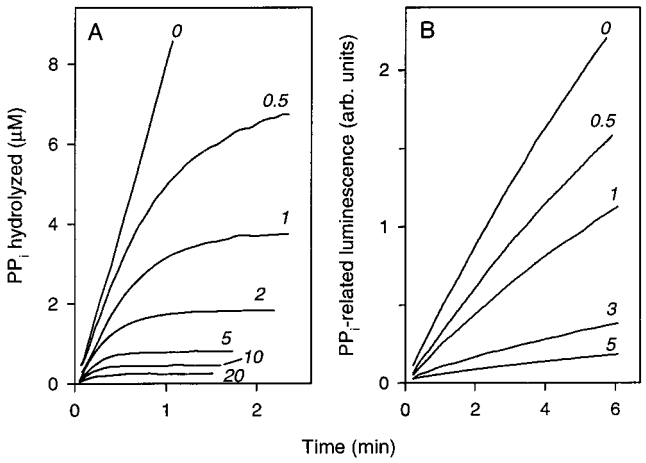


FIGURE 1: Effects of NaF on the progress curves for $PP_i$ hydrolysis (A) and $PP_i$ synthesis (B) catalyzed by Y-PPase at pH 7.2. One unit of luminescence corresponds to 1 $\mu$M $PP_i$ at zero time (luciferase fully active). NaF concentrations (mM) are indicated on the curves. Curves were normalized to 1.25 nM enzyme concentration.

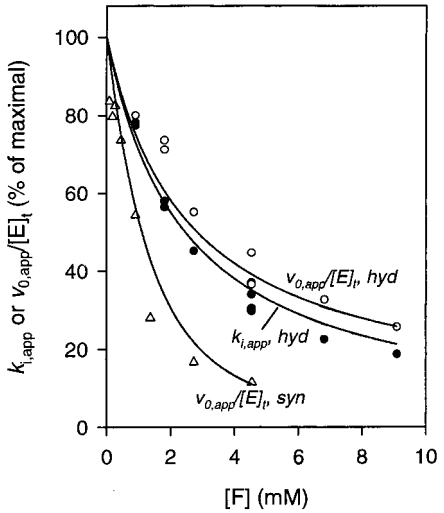


FIGURE 2: Dependence on $F^-$ concentration of the $v_{0,app}$ and $k_{i,app}$ values derived from the progress curves of $PP_i$ hydrolysis and synthesis by Y-PPase at pH 7.2. Lines were obtained with eqs 1 and 2 using parameter values found in Table 1 and the $n$ values indicated below. Open circles, $v_{0,app}$ for $PP_i$ hydrolysis ($n = 1$); triangles, $v_{0,app}$ for $PP_i$ synthesis ($n = 2$); filled circles, $k_{i,app}$ for $PP_i$ hydrolysis ($n = 1$).

fluoride concentrations (Figure 2). In contrast, the slow phase of PPase inactivation during enzymatic reaction was much slower in the synthesis reaction, as indicated by the straighter product formation curves at equal fluoride concentrations (Figure 1).

The dependence of $v_{0,app}$ and $k_{i,app}$ on inhibitor concentration estimated from $PP_i$ hydrolysis data with eqs 3 and 4 (Figure 1A) obeyed eqs 1 and 2, respectively, with very similar $K_{F1}$ values (Figure 2), and thus agreed with Scheme 2. The numerical values of all parameters controlling fluoride inhibition of PPase in the hydrolysis reaction were obtained by simultaneously fitting all curves in Figure 1A to eqs 1−4, and are listed in Table 1. At the higher pH value the inhibition of $PP_i$ hydrolysis is weaker in terms of both $k_{i,0}$ and $K_{F1}$, and $v_0'$ is smaller.

In the synthesis reaction, only $v_{0,app}$ values, but not $k_{i,app}$ values, could be estimated with eqs 3 and 4 from the product formation curves shown in Figure 1B, because of difficulty with spontaneous inactivation of luciferase, indicated by the nonlinear luminescence versus time curve in the absence of fluoride (Figure 1B). In contrast to the hydrolysis data, the $v_{0,app}$ versus [F] profile could be described only poorly by eq 1 with $n = 1$, and necessitated the use of $n = 2$, indicating that two fluoride ions are bound. The general form of the denominator of eq 1 in this case is $1 + a[F] + b[F]^2$, where $a$ and $b$ are constants. However, the fitting indicated that the term $a[F]$ is insignificant, which means that the two fluoride ions are bound in a strongly cooperative manner.

*Inactivation of Y-PPase Equilibrated with $P_i$.* Strong support for the binding of two $F^-$ ions to Y-PPase was obtained by measuring Y-PPase inactivation in the equilibrated $PP_i \rightleftharpoons P_i$ system (Figure 3). In these experiments, Y-PPase was incubated with fluoride, $P_i$, and $Mg^{2+}$ in the absence of the enzyme-coupled system used in $PP_i$ synthesis measurements. At the high enzyme concentration used, the $PP_i \rightleftharpoons P_i$ reaction in solution (but not on the enzyme) came to equilibrium during the first seconds of incubation, both in the absence and in the presence of fluoride. Aliquots of the incubation mixture were withdrawn and diluted 900−4500-fold with the assay mixture, and the residual hydrolytic activity was measured, giving the data shown in Figure 3. Because of the extensive dilution, the rapid phase of the inactivation was reversed, and thus only the extent of the slowly reversible phase governed by $k_{i,app}$ was measured. The final value of $\alpha$, corresponding to equilibrium between enzyme and $F^-$ [$\alpha_{eq} = 1/(1 + k_{i,app}[F]/k_r)$], exhibited a bell-shaped dependence on [F] (Figure 3, inset). In contrast, eq 2 predicts a monotonical change in $\alpha_{eq}$ at $n = 1$, which implies binding of only one fluoride ion. A satisfactory fit to the data shown in Figure 3 was obtained when eq 1 was used in combination with eq 2, in which $n$ was set to 2. The value of $K_{F1}$ estimated by this fitting (Table 1) agrees with the value derived from the analysis of $PP_i$ synthesis in solution.

An identical analysis of fluoride inhibition was performed at 2 mM $P_i$ concentration (data not shown). The results were qualitatively similar, but the maximum degree of inhibition (observed again at 1 mM fluoride) was only 50%. This resulted from a 9-fold decrease in $k_{i,0}$. Significantly, the value

Table 2: pH Dependence of Y-PPase Inactivation and Enzyme-Bound $PP_i$ Formation in the Presence of Fluoride[a]

| | | | inactivation[b] | | enzyme-bound $PP_i$ formation[c] | | |
|---|---|---|---|---|---|---|---|
| pH | $[Mg^{2+}]$ (mM) | $[P_i]$ (mM) | $k_{i,app}$ ($mM^{-1}\cdot min^{-1}$) | $k_r$ ($min^{-1}$) | $k_{i,app}$ ($mM^{-1}\cdot min^{-1}$) | $f_{epp,0}$ | $f_{epp}^{fast}$ |
| 4.8 | 40 | 40 | 0.070 ± 0.004 | 0.010 ± 0.001 | 0.081 ± 0.003 | 0.010 ± 0.002 | 0.0085 ± 0.0024 |
| 5.5 | 20 | 20 | 0.064 ± 0.011 | 0.0087 ± 0.003 | 0.070 ± 0.004 | 0.043 ± 0.003 | 0.018 ± 0.004 |
| 6.3 | 20 | 20 | 0.157 ± 0.010 | 0.015 ± 0.002 | 0.105 ± 0.013 | 0.193 ± 0.006 | 0.074 ± 0.015 |
| 7.2 | 5 | 20 | 0.030 ± 0.002 | 0.016 ± 0.003 | 0.017 ± 0.001 | 0.16 ± 0.02 | 0.053 ± 0.005 |
| 8.5 | 5 | 10 | | | <0.0002 | 0.153 ± 0.007 | 0.011 ± 0.002 |
| | | | | | (0.9 ± 0.2)[d] | | (0.063 ± 0.006)[d] |

[a] NaF concentration was 1 mM (pH 4.8) or 2 mM (other pH values). [b] Parameters obtained with eq 4. [c] Parameters, except for $f_{epp,0}$, obtained with eqs 5 and 6. [d] Determined from the time course of $f_{epp}$ decline.

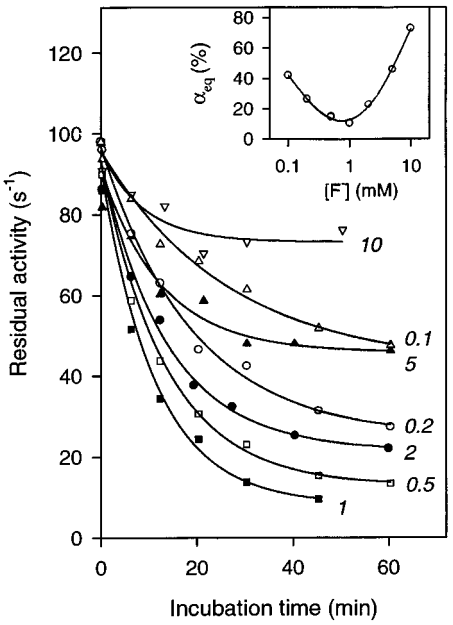


FIGURE 3: Time-courses of Y-PPase inactivation during incubation with NaF in the presence of 5 mM free $Mg^{2+}$ and 20 mM total $P_i$ at pH 7.2. NaF concentrations (mM) are indicated on the curves. The reaction was carried out at 25 °C in a total volume of 70 $\mu$L at 3.6 $\mu$M enzyme concentration. Aliquots of 2−12 $\mu$L were withdrawn at the indicated time intervals, and the residual activity of PPase was measured in medium containing 1 mM $PP_i$, 0.2 mM $MgCl_2$, 10 $\mu$M EGTA, and 0.05 M Tris-HCl, pH 8.5. Lines were obtained with eqs 2 ($n = 2$) and 4 using parameter values found in Table 1. Inset: the residual activity of Y-PPase at infinite time ($\alpha_{eq}$) as a function of $F^-$ concentration.

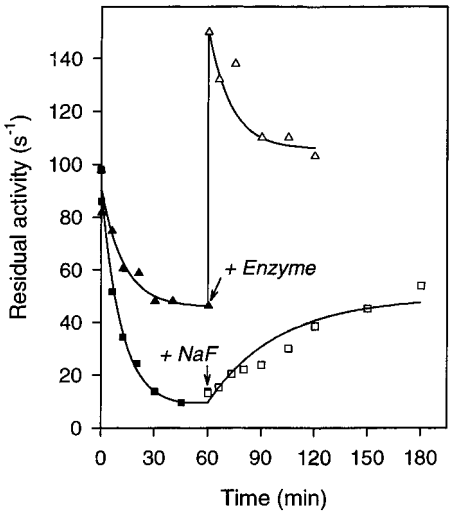


FIGURE 4: Controls demonstrating no fluoride ion sequestration because of $MgF_2$ precipitation in the experiments shown in Figure 3. After 60 min incubation with 1 mM NaF (closed squares) or 5 mM NaF (closed triangles) under conditions identical to those used for Figure 3, an additional 9 mM NaF (open squares) or an equal amount of fresh Y-PPase (open triangles) was added, and activity changes were followed for a further 60 min. The lines were obtained with eqs 2 ($n = 2$) and 4 as for Figure 3, taking into account changes in enzyme and inhibitor concentrations. 100% activity refers to the enzyme initially present in the incubation mixtures.

of $K_{F1}$ was only slightly changed between 2 and 20 mM $P_i$ concentrations (Table 1).

A more trivial explanation of the unusual effect of $F^-$ concentration on the inactivation seen in Figure 3 could be sequestration of $F^-$ because of $MgF_2$ formation during the incubation, to the extent that its solubility product ($10^{-8.2}$ $M^3$; *30*) was exceeded at ≥2 mM $F^-$. However, earlier measurements done with an $Mg^{2+}$-sensitive electrode indicated that $MgF_2$ is formed quite slowly on the time scale of the assays (*31*). The data shown in Figure 4 provide further support for this contention. Addition of fresh enzyme to the system equilibrated at 5 mM NaF resulted in an identical inactivation profile, whereas addition of 9 mM NaF to the system equilibrated at 1 mM NaF resulted in partial reactivation, approaching the level observed in the forward reaction at 10 mM $F^-$ (Figure 3).

The value of $k_{i,app}$ was pH-dependent (Table 2). No inactivation was observed at pH 8.5, indicating a value of $k_{i,app}$ close to zero, because the value of $k_r$ (measured in $PP_i$ hydrolysis) is not changed between pH 7.2 and 8.5 (*18*, *31*; see also Table 1). The data in Table 2 show that $k_r$ remains virtually constant down to pH 4.8.

*Effect on Enzyme-Bound $PP_i$ Formation by Y-PPase*. About one-sixth of Y-PPase equilibrated with 20 mM $P_i$ and 5 mM $Mg^{2+}$ contained enzyme-bound $PP_i$ at both pH 7.2 and pH 8.5 (Figure 5), in agreement with published data (*9*, *14*, *32*). Addition of fluoride caused an instant (half-time <12 s) drop in the amount of the enzyme·$PP_i$ complex ($f_{epp}$) followed, at pH 7.2, by a gradual rise to a level similar to (10 mM NaF) or markedly exceeding (2 mM NaF) the level observed before the addition of NaF (Figure 5). Similar dependencies were obtained at pH 6.3, 5.5, and 4.8 (data not shown). At pH 7.2, the initial drop in $f_{epp}$ was larger at higher [F]. In contrast, no rise in $f_{epp}$ (<0.005 in 100 min) was observed at pH 8.5. Moreover, the initial drop clearly occurred in two steps: an instant (half-time <12 s) decrease to 0.079 ± 0.015 and a slower (half-time of 20 ± 5 s) decrease to 0.012 ± 0.002 (Figure 5, inset). The time-dependent rise in $f_{epp}$ at pH ≤7.2 can be approximated by eqs 5 and 6, where $f_{epp}^{fast}$ refers to the fraction of enzyme·$PP_i$ complex after completion of the fast phase of the interaction with $F^-$ (i.e., the zero-time point for the slow phase) and $f_{epp}^{slow}$ is the fraction of enzyme·$PP_i$ complex

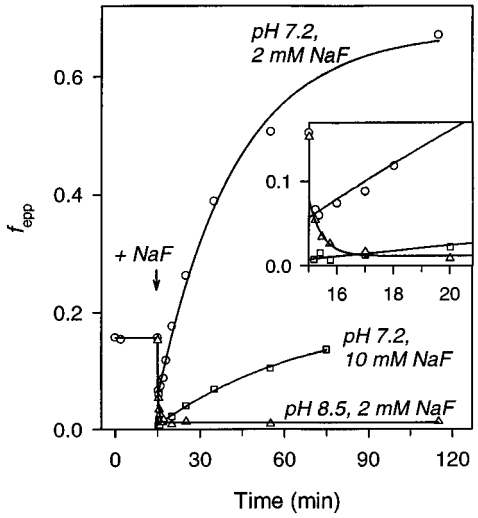


FIGURE 5: Time-courses of $f_{epp}$ upon addition of NaF to Y-PPase (0.13−0.16 mM) preequilibrated with 5 mM free $Mg^{2+}$ and 20 mM total $P_i$. Values of pH and NaF concentrations are indicated on the curves. The reaction was carried out at 25 °C in a total volume of 230 $\mu$L. Aliquots of 20 $\mu$L were withdrawn at the indicated time intervals, quenched with 4 $\mu$L of 5 M trifluoroacetic acid, and assayed for $PP_i$. The lines showing increase in $f_{epp}$ were calculated with eqs 5 and 6 using parameter values found in Table 2. Inset: same data on a different time scale. The line for pH 8.5 was obtained with the equation: $f_{epp} = f_{epp}^{fast} + (f_{epp}^{int} - f_{epp}^{fast})e^{-kt}$, where $f_{epp}^{fast} = 0.012$, $f_{epp}^{int} = 0.079$, and $k = 1.8$ min$^{-1}$.

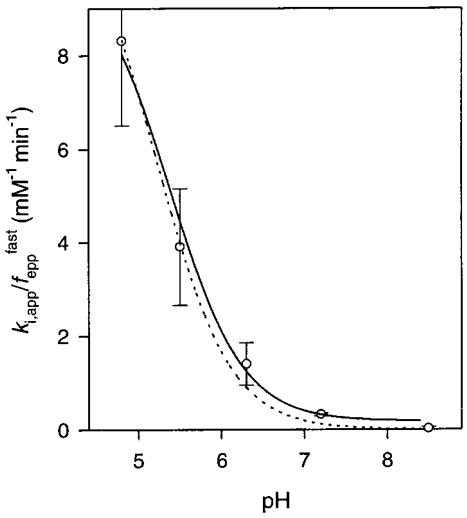


FIGURE 6: pH-dependence of $k_{i,app}/f_{epp}^{fast}$ calculated from the data on $EPP_i$ formation shown in Table 2. See text for details.

accumulated at time $t$ during the slow phase. The values of $k_{i,app}$ and $f_{epp}^{fast}$ thus obtained are summarized in Table 2. Values of $k_r$ were too small to be estimated in this way and were thus constrained to the values determined above from PPase inactivation (Table 2).

$$f_{epp} = f_{epp}^{slow} + f_{epp}^{fast}(1 - f_{epp}^{slow}) \quad (5)$$

$$\frac{df_{epp}^{slow}}{dt} = k_{i,app}[F^-](1 - f_{epp}^{slow}) - k_r f_{epp}^{slow} \quad (6)$$

The slow rise in $f_{epp}$ clearly reflects fluoride binding to enzyme·$PP_i$ complex, the true rate constant for this reaction being $k_{i,app}/f_{epp}^{fast}$. Its pH-dependence (Figure 6) can be described by a curve for a single ionization with a p$K_a$ of 5.4 ± 0.2 and limiting values of $k_{i,app}/f_{epp}^{fast}$ of 0.17 ± 0.04 and 10 ± 2 mM$^{-1}$·min$^{-1}$ in the alkaline and acidic regions, respectively. Assuming zero limit in the alkaline region (dotted curve) led to a poorer fit to the points measured at pH 6.3 and 7.2.

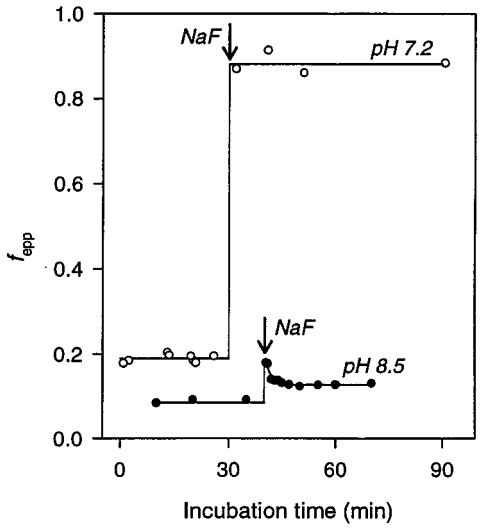


FIGURE 7: Time-courses of $f_{epp}$ upon addition of 2 mM NaF to *E. coli* PPase (30−140 $\mu$M) preequilibrated with 5 mM free $Mg^{2+}$ and 20 mM total $P_i$ (pH 7.2) or 10 mM total $P_i$ (pH 8.5). Other conditions were as for Figure 5. The arrows mark the moments of fluoride addition. Open symbols, pH 7.2; closed symbols, pH 8.5.

*Identification of Y-PPase Species Stabilized by F$^-$ during Hydrolysis at pH 8.5.* At pH 7.2, the slow phase of Y-PPase inactivation in both hydrolysis (*17*) and synthesis (see above) corresponds to $F^-$ binding to the enzyme·$PP_i$ complex. No slow inhibition phase was observed at pH 8.5 in the presence of $P_i$; moreover, a slow binding of $F^-$ to an enzyme·$P_i$ intermediate was detected (Figure 5, inset), presenting the possibility that this binding is responsible for the slow inactivation of Y-PPase during $PP_i$ hydrolysis at pH 8.5 (Table 1). This was tested by measuring the $PP_i$ content of Y-PPase inactivated at pH 8.5 in the presence of $PP_i$. After a 3 min incubation of 6.3 $\mu$M enzyme with 1 mM $PP_i$ in the presence of 5 mM $MgCl_2$, the $PP_i$ concentration dropped to its equilibrium value of 0.6 $\mu$M, consistent with high catalytic activity of Y-PPase. If, however, 10 mM NaF was present during this incubation, the concentration of the remaining $PP_i$ was significantly higher (2.9 $\mu$M), and the enzyme was inactivated by 20%. Further incubation for 3 min upon addition of the same amount of fresh enzyme only slightly decreased the $PP_i$ level (to 2.2 $\mu$M). These data show that $F^-$ mediated the incorporation of 1.6 $\mu$M $PP_i$ into Y-PPase, which corresponds to 25% of the total enzyme. The latter value correlates with the degree of enzyme inactivation. Thus, the slow inactivation of Y-PPase during hydrolysis results from fluoride binding to the enzyme·$PP_i$ complex at both pH 7.2 and pH 8.5.

*Fluoride Effects on E-PPase.* Addition of NaF to E-PPase preequilibrated with $P_i$ caused a rapid rise (half-time <15 s) in $f_{epp}$ at pH 7.2 and 8.5 (Figure 7), indicating $F^-$ binding to an enzyme·$PP_i$ complex. At pH 8.5, the rise was followed by a slower decline, showing that $PP_i$-free enzyme also binds $F^-$, but at a lower rate. The final equilibrium level of $f_{epp}$ exhibited a bell-shaped dependence on fluoride concentration (Figure 8). At pH 8.5, the final level measured at high

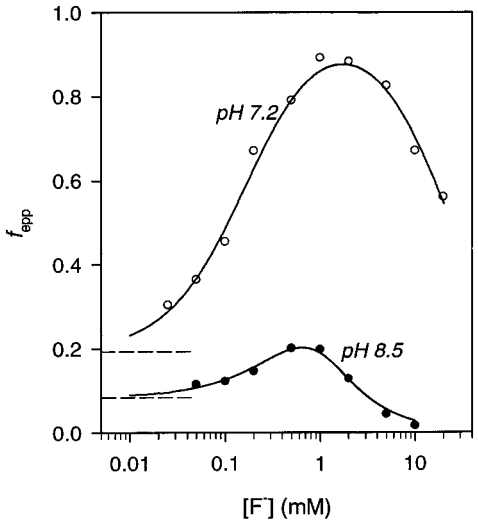


FIGURE 8: Equilibrium value of $f_{epp}$ for *E. coli* PPase as a function of fluoride concentration at two pH values. The lines were obtained with eq 7, using parameter values found in Table 3.

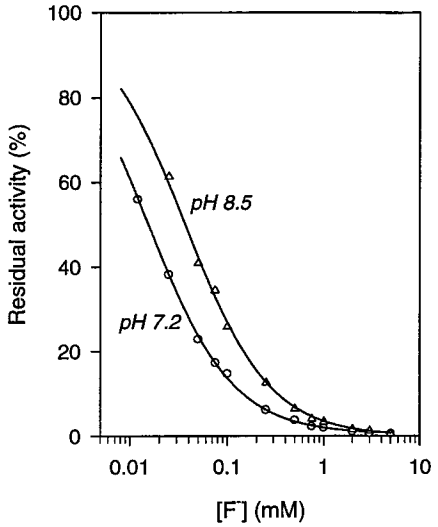


FIGURE 9: Fluoride inhibition of *E. coli* PPase at two pH values. At each pH value, 100% refers to the activity measured in the absence of fluoride. The lines were obtained with eq 1, in which $K_{F1}$ was replaced by $K_I$, using $n = 1$ and parameter values found in Table 3.

Table 3: Parameters for Fluoride Binding to *E. coli* PPase

| | enzyme-bound $PP_i$ formation | | | inhibition of hydrolysis |
|---|---|---|---|---|
| pH | $K_{F1}$ ($mM^2$) | $K_{F2}$ (mM) | $f_{epp,0}$ | $K_I$ ($\mu$M) |
| 7.2 | $3.2 \pm 0.2$ | $0.16 \pm 0.01$ | $0.19 \pm 0.01$ | $15 \pm 1$ |
| 8.5 | $0.50 \pm 0.05$ | $1.9 \pm 0.2$ | $0.086 \pm 0.003$ | $37 \pm 1$ |

fluoride concentration was below the level measured without fluoride, indicating greater fluoride binding affinity of the $PP_i$-free enzyme compared to the enzyme·$PP_i$ complex. The dependencies of $f_{epp}$ on [F] at equilibrium can be fit with eq 7, yielding the dissociation constants $K_{F1}$ and $K_{F2}$, governing fluoride binding to $PP_i$-free enzyme and the enzyme·$PP_i$ complex, respectively; as well as $f_{epp,0}$, the value of $f_{epp}$ in the absence of fluoride (Table 3). Equation 7 assumes that the enzyme·$PP_i$ complex binds one and the $PP_i$-free enzyme binds two $F^-$ ions; otherwise, a bell-shaped $f_{epp}$ profile, such as seen in Figure 8, would not be obtained. Sequestration of fluoride by its binding with the enzyme was taken into account when fitting eq 7 to the data in Figure 8.

$$f_{epp} = \frac{1}{1 + \dfrac{(1/f_{epp,0} - 1)(1 + [F]^2/K_{F1})}{1 + [F]/K_{F2}}} \qquad (7)$$

$F^-$ inhibition of E-PPase during $PP_i$ hydrolysis was attained rapidly at both pH 7.2 and pH 8.5, confirming earlier data (*19*, *20*). The inhibition was observed at relatively low fluoride concentrations, and the dependence of activity on [F] was hyperbolic (Figure 9), indicating binding of only one $F^-$ ion. These features of the inhibition suggest that fluoride mainly binds to an enzyme·$PP_i$ species. The value of the inhibition constant $K_I$, estimated from the data in Figure 9 with an equation similar to eq 1 with $n = 1$ but using $K_I$ instead of $K_{F1}$, was less by a factor of 11 at pH 7.2 and by 51 at pH 8.5 than the corresponding value of $K_{F2}$ obtained from the effect on $f_{epp}$ (Table 3).

## DISCUSSION

*Kinetic Scheme of Inhibition.* Earlier studies have established that fluoride inhibition of $PP_i$ hydrolysis by yeast and rat liver PPases occurs in two phases—fast and slow, and that a $PP_i$ molecule is trapped in the active site in the slow phase (*13*, *14*). It was suggested that the two phases reflect fluoride binding to the enzyme·$PP_i$ intermediate and isomerization of the resulting ternary complex, respectively. The results of the present study provide a different explanation of the unusual time-course of inhibition, as shown in Scheme 3. Its salient feature is that the slow and the fast phases of the inhibition are bimolecular binding reactions involving different enzyme species—enzyme·$PP_i$ and enzyme·$P_i$ complexes, respectively. Furthermore, Scheme 3 differs from Scheme 1 in having two enzyme·$PP_i$ intermediates (one of these can be protonated).

Slow binding of fluoride to the enzyme·$PP_i$ complex is indicated by its accumulation in the reaction medium in the presence of Mg−$PP_i$ (*17*) or Mg−$P_i$ (Figure 5). In contrast, the amount of the enzyme·$PP_i$ complex is *decreased* during the fast phase of the interaction with fluoride in the Mg−$P_i$ system (Figure 5). This can only happen if fluoride binds to an enzyme species lacking bound $PP_i$, and thus decreases the amount of enzyme available to form the $PP_i$ complex. There are three such species in Scheme 3: $EM_2$, $EM_{n+2}P_2$, and $EM_{n+1}P$. From the Michaelis constant of 0.8 $\mu$M for $PP_i$, the dissociation constants governing successive binding of two $MgP_i$ molecules to Y-PPase (0.62 and 2.7 mM; *34*), and the equilibrium constant $[EM_{n+2}P_2]/([EM_{n+2}PP^*] + [HEM_{n+2}PP^*]) = 4.65$ (*33*), one can calculate that $EM_2$ accounts for <2% of the total enzyme under the conditions used for Figures 1A and 5. Keeping in mind the rather low affinity of $EM_2$ for $F^-$ ($K_d \sim 3$ mM; *13*), one can thus conclude that $EM_2$ does not contribute significantly to the observed fluoride binding. Furthermore, considering that a 10-fold change in $P_i$ concentration at pH 7.2 had only a small effect on $K_{F1}$ (Table 1), it is more likely that $EM_{n+1}P$, and not $EM_{n+2}P_2$, binds fluoride during the fast phase of inhibition. From the values of the $MgP_i$ binding constants listed above, one can calculate that the fraction of $EM_{n+2}P_2$ decreases from 59 to 11% and that of $EM_{n+1}P$ increases from 26 to 47% when the $P_i$ concentration is decreased from 20 to 2 mM. The effect of $P_i$ concentration on $K_{F1}$ thus correlates

Scheme 3: $PP_i$-$P_i$ Equilibration by Y-PPase and Its Inhibition by Fluoride[a]

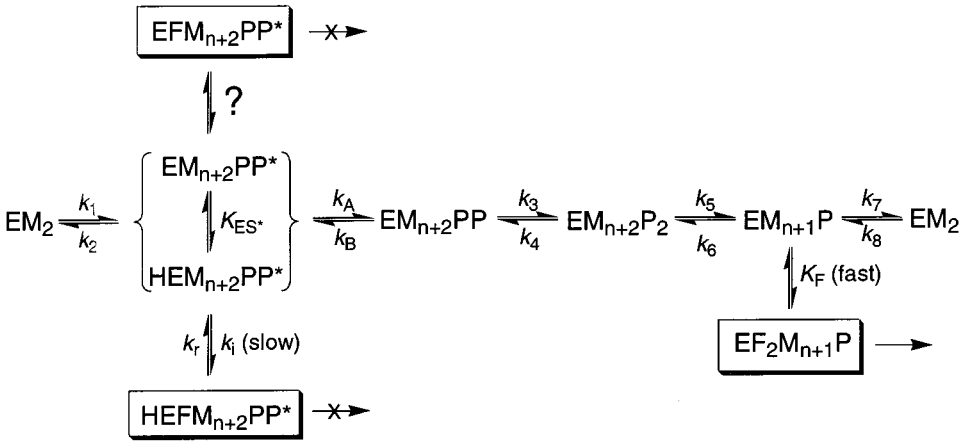


$k_1 = 3.8 \cdot 10^8\ M^{-1} \cdot s^{-1}$
$k_2 = 1600\text{-}4100\ s^{-1}$
$k_A = 840\text{-}2200\ s^{-1}$
$k_B = 34\text{-}33\ s^{-1}$
$k_3 = 1400\ s^{-1}$
$k_4 = 350\ s^{-1}$
$k_5 = 800\ s^{-1}$
$k_6 = 3 \cdot 10^5\ M^{-1} \cdot s^{-1}$
$k_7 = 3300\text{-}960\ s^{-1}$
$pK_{ES^*} > 7.0$
$k_i = 10\ mM^{-1} \cdot min^{-1}$
$k_r = 0.016\ min^{-1}$
$K_F = 0.17\text{-}0.42\ mM^2$

[a] The fluoride complex of $EM_{n+1}P$ corresponds to the complex formed in the Mg−$P_i$ system. Values for the rate constants and $K_F$ are for pH 7.2; values of $k_3$−$k_6$ are from Baykov and Shestakov (*33*).

better with its effect on the amount of $EM_{n+1}P$, although the possibility that $EM_{n+1}P_2$ also has some affinity for fluoride cannot be excluded.

During the fast phase, two fluoride ions are bound to Y-PPase in the presence of $P_i$, but only one is bound in the presence of $PP_i$. This could result if the second $F^-$ ion is inhibitory in $PP_i$ synthesis but not in $PP_i$ hydrolysis, and this explanation is consistent with $k_s$ and $k_h$ being controlled by different rate constants (Scheme 3). Another possibility is that the time needed for the second $F^-$ ion to bind is greater than the lifetime of the $EM_{n+1}P$ species (which is in the millisecond range) in the hydrolysis reaction. That the "fast" phase is not extremely fast is indicated by the fact that its time course is clearly resolved at pH 8.5 (Figure 5).

The data measured for E-PPase are also consistent with Scheme 3. Fluoride addition to E-PPase preequilibrated with $MgP_i$ at pH 8.5 (Figure 7) results in a rapid rise in $f_{epp}$ (fluoride binding to an enzyme·$PP_i$ complex) followed by its slow decline (fluoride binding to an enzyme species lacking bound $PP_i$, presumably an enzyme·$P_i$ complex). The two enzymes differ in that the enzyme·$PP_i$ species binds fluoride slowly in Y-PPase (Figure 5) and rapidly in E-PPase (Figure 7). In contrast, the enzyme·$P_i$ species behave similarly in the two PPases: they bind instantly at pH 7.2 and with a measurable rate at pH 8.5 (Figures 5 and 7). As with Y-PPase, the E-PPase enzyme·$P_i$ species binds more $F^-$ ions than the enzyme·$PP_i$ species; otherwise the equilibrium levels of $f_{epp}$, rather than passing through a maximum (Figure 8), would monotonically increase or decrease with [F], depending on the relative affinities of the enzyme·$PP_i$ and enzyme·$P_i$ species.

*A Second Enzyme·$PP_i$ Intermediate.* Perhaps the most important finding of the present study is that the enzyme·$PP_i$ complexes formed in the Mg−$P_i$ and Mg−$PP_i$ systems display different reactivity toward fluoride. The true rate constant for fluoride binding to this species in the Mg−$P_i$ system ($k_{i,app}/f_{epp}^{fast}$) is 0.32−0.57 $mM^{-1}$·$min^{-1}$ at pH 7.2 (the upper limit was obtained from the $k_{i,app}$ value derived from enzyme inactivation) and <0.02 $mM^{-1}$·$min^{-1}$ at pH 8.5 (Table 2). The corresponding rate constant in the Mg−$PP_i$ system is given by $k_{i,0}/f_{epp,ss}$, where $f_{epp,ss}$ is the fraction of the enzyme containing bound $PP_i$ during steady-state hydrolysis. As $f_{epp,ss}$ is less than unity, $k_{i,0}/f_{epp,ss}$ is greater than $k_{i,0}$, i.e., 2.7 and 0.94 $mM^{-1}$·$min^{-1}$ at pH 7.2 and 8.5, respectively (Table 1). For E-PPase, the apparent affinities of the enzyme·$PP_i$ complexes to fluoride measured in the Mg−$P_i$ and Mg−$PP_i$ systems differ 11-fold at pH 7.2 and 51-fold at pH 8.5, whereas the *amounts* of these complexes differ in the two systems less than 5.3-fold and 12-fold, respectively (these upper limits were estimated assuming $f_{epp,ss} = 1$) (Table 3).

The only explanation for this apparent discrepancy is that there are at least two enzyme·$PP_i$ intermediates reacting with fluoride with substantially different rates and/or affinities (we assumed that one does not react at all) and that the fraction of the more reactive intermediate in the total pool of the enzyme·$PP_i$ intermediates is greater during steady-state hydrolysis than at equilibrium with $P_i$. The steady-state concentration of each intermediate in a reaction involving several consecutive steps, like that shown in Scheme 3, is less than predicted by its equilibrium with the *preceding* intermediate. Therefore, only $EM_{n+2}PP^*$ (together with its protonated form $HEM_{n+2}PP^*$) can be present at a concentration exceeding that required by the equilibrium governed by $K_{AB} = k_A/k_B$ during steady-state hydrolysis. This idenifies this intermediate as the target for fluoride in the slow phase, and the pH-dependence shown in Figure 6 suggests that $HEM_{n+2}PP^*$ is the major binding species at pH <7. $EM_{n+2}PP^*$ may also bind fluoride if the limiting value of $k_{i,app}/f_{epp}^{fast}$ at high pH in Figure 6 (0.17 $mM^{-1}$·$min^{-1}$) refers to

this species, but this value may also refer to $EM_{n+2}PP$. Equilibrium between $EM_{n+2}PP^*$ and $HEM_{n+2}PP^*$ appears to be always attained because this conversion is not on the main reaction route. Independent support for Scheme 3 comes from recent pre-steady-state measurements of $PP_i$ hydrolysis by Y-PPase, which also indicated two enzyme·$PP_i$ intermediates (Halonen et al., manuscript in preparation).

*Rate and Equilibrium Constants for Scheme 3.* The observation of a second enzyme·$PP_i$ intermediate has important consequences for the determination of the rate constants for the individual catalytic steps of PPase catalysis. The currently used procedure (*28*) was formulated for Scheme 1 which has only one such intermediate. This procedure relies heavily on measurements of $[^{18}O]P_i-[^{16}O]$-$H_2O$ oxygen exchange and enzyme-bound $PP_i$ formation, and starts from $k_3$ calculation. Oxygen exchange measurements yield two important parameters: the rate of the exchange ($v_{ex}/[E]_t$) and the partition coefficient, $P_c = k_4/(k_4 + k_5)$, which is calculated from the distribution of five $P_i$ species having from zero to four $^{18}O$ atoms during the exchange (*35*). For Scheme 3, the expressions for $v_{ex}/[E]_t$ (*36*) and $f_{epp}$ are given by eqs 8 and 9:

$$\frac{v_{ex}}{[E]_t} = \frac{k_5 K_3 P_c}{(1 + K_3 + 1/K_{AB})(1 - 0.75P_c)\Sigma} \quad (8)$$

$$f_{epp} = \frac{1 + 1/K_{AB}}{(1 + K_3 + 1/K_{AB})\Sigma} \quad (9)$$

where $\Sigma = 1 + (K_3K_5/[MP] + K_3K_5K_7/[MP]^2)/(1 + K_3 + 1/K_{AB})$, $K_3 = k_3/k_4$, $K_5 = k_5/k_6$, $K_7 = k_7/k_8$, and $K_{AB} = [EM_{n+2}PP]/([EM_{n+2}PP^*] + [HEM_{n+2}PP^*])$. From eqs 8 and 9 and the expression for $P_c$, eq 10 can be derived, which differs from the equation previously used to estimate $k_3$ (*28*) by having a $(1 + 1/K_{AB})$ term in the numerator. Knowledge of $K_{AB}$ is thus required for $k_3$ determination.

$$k_3 = \frac{v_{ex}(1 - 0.75P_c)(1 + 1/K_{AB})}{f_{epp}(1 - P_c)[E]_t} \quad (10)$$

In contrast, values of $k_4$ and $k_5$ can be estimated without knowing $K_{AB}$. The value of $k_4$ is equal to $k_3/K_3$, where $K_3$ is obtained from $f_{epp}^{lim}$, the limiting value of $f_{epp}$ at infinite [MP] ($\Sigma = 1$ in eq 9), as $(1/f_{epp}^{lim} - 1)(1 + 1/K_{AB})$. From this and eq 10, one gets eq 11 for $k_4$. This, in turn, allows calculation of $k_5$ from $P_c$. Finally, $k_6$ is calculated as $k_5/K_5$, where $K_5$ is obtained from the saturation function $\Sigma$ for $v_{ex}/[E]_t$ (eq 8) or $f_{epp}$ (eq 9). Up to this point, all the calculations employed only parameter values measured under equilibrium conditions. Values of $k_7$ (and hence $k_8$) cannot be calculated from measured $k_h$, as was done previously (*32*), because $k_h$ will also depend on $k_A$ and $k_B$ (eq 12); the same applies to the calculations of $k_1$ from $k_h/K_{m,h}$ and of $k_2$ from $k_s$ (see eqs 13 and 14, respectively). In eqs 12 and 13, $k_A$ and $k_2$ are the apparent rate constants referring to the sum of $EM_{n+2}PP^*$ and $HEM_{n+2}PP^*$. Equations 12−14 were derived using the method of net rate constants (*37, 38*).

$$k_4 = \frac{v_{ex}(1 - 0.75P_c)}{f_{epp}(1 - P_c)(1/f_{epp}^{lim} - 1)[E]_t} \quad (11)$$

$$\frac{1}{k_h} = \frac{1}{k_A} + \frac{1 + 1/K_{AB}}{k_3(1 - P_c)} + \frac{1}{k_5} + \frac{1}{k_7} \quad (12)$$

$$\frac{k_h}{K_{m,h}} = \frac{k_1 k_A}{k_2[1 + k_B/k_3(1 - P_c)]} \quad (13)$$

$$\frac{1}{k_s} = \frac{1 + K_{AB} + K_{AB}K_3}{k_2} + \frac{1 + K_3}{k_B} + \frac{1}{k_4} \quad (14)$$

Thus, in summary, the previous estimates of $k_4$ (222−350 $s^{-1}$), $k_5$ (740−800 $s^{-1}$), and $k_6$ ($1.64 \times 10^5$ to $3 \times 10^5$ $M^{-1}\cdot s^{-1}$) (*32, 33*) are true, and the estimate of $k_3$ (1070−1400 $s^{-1}$) is true provided that $K_{AB} \gg 1$, but the previous estimates of $k_1$, $k_2$, $k_7$, and $k_8$ need to be reconsidered.

The estimation of the latter four constants, as well as estimation of $k_A$ and $k_B$, requires additional information, which can be extracted from the fluoride inhibition data. We will illustrate this by making calculations for Y-PPase using the data previously collected at pH 7.2, 5 mM $Mg^{2+}$, and 0.1 M ionic strength (*33*), i.e., under conditions used in this work. In the presence of 2 mM NaF at pH 7.2, the fraction of $HEM_{n+2}PP^*$ in the total pool of the enzyme·$PP_i$ complexes at equilibrium with $P_i$ in solution can be calculated as $(0.32 - 0.17)/(10 - 0.17) = 0.0153$, where 0.32 is the value of $k_{i,app}/f_{epp}^{fast}$ at pH 7.2 (Table 2), and 10 and 0.17 are the limiting values of $k_{i,app}/f_{epp}^{fast}$ at low and high pH values (Figure 6). Since the total fraction of enzyme·$PP_i$ complexes is 0.053 under these conditions (see $f_{epp}^{fast}$ in Table 2), the contribution of $HEMn_{+2}PP^*$ will be $0.0153 \times 0.053 = 0.00081$. The value of $k_{i,0}$ in hydrolysis (2.7 $mM^{-1}\cdot min^{-1}$) is greater by a factor of 159 than $k_{i,app}$ at equilibrium with $P_i$ (0.017 $mM^{-1}\cdot min^{-1}$); hence, the fraction of $HEM_{n+2}PP^*$ is $0.00081 \times 159 = 0.129$ in hydrolysis. The fraction of $EM_{n+2}PP^*$ cannot then exceed $1 - 0.129 = 0.871$, and, accordingly, the ratio $[EM_{n+2}PP^*]/[HEM_{n+2}PP^*]$ must be smaller than $0.871/0.126 = 6.75$. The latter estimate is also applicable to the $Mg^{2+}-P_i$ system, leading to $[EM_{n+2}PP^*]/[E]_t < 0.00081 \times 6.75 = 0.0055$ and, accordingly, $[EM_{n+2}PP]/[E]_t < 0.053 - 0.00081 - 0.0055 = 0.0467$. Therefore, the lower and upper limits of $K_{AB} = [EM_{n+2}PP]/([HEM_{n+2}PP^*] + [EM_{n+2}PP^*])$ are 7.4 ($[HEM_{n+2}PP^*]/[E]_t = 0.00081$, $[EM_{n+2}PP^*]/[E]_t = 0.0055$) and 65 ($[HEM_{n+2}PP^*]/[E]_t = 0.00081$, $[EM_{n+2}PP^*]/[E]_t = 0$), respectively. Allowing $K_{AB}$ to change stepwise between these limits and using the previous estimates of $k_3$ (1400 $s^{-1}$), $k_4$ (350 $s^{-1}$), and $k_5$ (800 $s^{-1}$) together with the measured value of $P_c$ (0.35) (*33*), we found pairs of $k_A$ and $k_7$ values simultaneously yielding $k_h$, the catalytic constant for hydrolysis, of 259 $s^{-1}$ and $[HEM_{n+2}PP^*]/[E]_t$ of 0.129 at each $K_{AB}$ value for Scheme 3. These simulations were done with the program Berkeley Madonna of R. I. Macey and G. F. Oster (available at www.berkeleymadonna.com). Finally, $k_2$ values corresponding to each pair of $k_A$ and $k_7$ values were obtained with eq 13, using $k_s$, the catalytic constant for synthesis, of 4.2 $s^{-1}$ (*33*), and the corresponding $k_1$ values were obtained with eq 13. At $K_{AB} < 25$, negative values of $k_2$ were obtained, narrowing the permissible $K_{AB}$ range to 25−65. The values of all parameters obtained in this way are summarized in Scheme 3. The values of $k_1$ and $k_6$ are given in terms of total $PP_i$ and $MgP_i$ concentrations, respectively. Where ranges of parameters are shown, the first value is for $K_{AB} = 25$ and the second for

$K_{AB} = 65$. All the parameters changed monotonically within their ranges. From $K_{AB} > 25$, one could calculate ($[HEM_{n+2}PP^*] + [EM_{n+2}PP^*]$)/$[E]_t$ to be <0.00204 [0.053/(25 + 1)] and, hence, $[EM_{n+2}PP^*]/[E]_t < 0.00125$ at equilibrium with $P_i$, setting the lower limit of $pK_{ES^*}$ at 7.0.

The value for the dissociation constant $K_F = 0.17-0.42$ $mM^2$ for the difluoride complex of $EM_{n+1}P$ in Scheme 3 was obtained by multiplying the value of $K_{F1}$ by the fraction of enzyme present as $EM_{n+1}P$ at equilibrium with $P_i$ (0.26; see above). In the hydrolysis reaction, only one fluoride ion is bound, and the dissociation constant of 0.19−0.62 mM for the resulting complex can be calculated from the value of $K_{F1}$ (Table 1) and the fraction of enzyme present as $EM_{n+1}P$ during steady-state hydrolysis (0.081−0.27, as obtained in the simulations). For comparison, the dissociation constant for the monofluoride complex of $HEM_{n+2}PP^*$ ($k_r/k_i$) is only 1.6 $\mu$M.

The values of the parameters obtained allow the following conclusions to be made: (a) Values of $k_A$, $k_3$, $k_5$, and $k_7$ are similar, which means that the concentrations of the reaction intermediates present during hydrolysis are nearly equal. This distinguishes PPase as a highly efficient catalyst. (b) Consistent with this, the value of $k_h/K_{m,h}$ ($3.8 \times 10^8$ $M^{-1}\cdot s^{-1}$) is greater than for any of the most efficient enzymes recently tabulated by Fersht (*38*). (c) In the direction of synthesis, the $k_B$ step is exclusively rate-limiting at saturating magnesium phosphate concentration. Accordingly, the asterisked species are present in only small amounts (1−3% of the total enzyme), and the ratio of the dominant species, $[EM_{n+2}P_2]/[EM_{n+2}PP]$, is very close to $K_{AB}$.

## REFERENCES


1. Kornberg, A. (1962) in *Horizons in Biochemistry* (Kasha, M., and Pullman, B., Eds.) p 251, Academic Press, New York.
2. Cooperman, B. S., Baykov, A. A., and Lahti, R. (1992) *Trends Biochem. Sci. 17*, 262−266.
3. Baykov, A. A., Cooperman, B. S., Goldman, A., and Lahti, R. (1999) *Prog. Mol. Subcell. Biochem. 23*, 127−150.
4. Kunitz, M. (1952) *J. Gen. Physiol. 35*, 423−450.
5. Baykov, A. A., and Avaeva, S. M. (1973) *Eur. J. Biochem. 32*, 136−142.
6. Welsh, K. M., Jacobyansky, A., Springs, B., and Cooperman, B. S. (1983) *Biochemistry 22*, 2243−2248.
7. Baykov, A. A., Shestakov, A. S., Kasho, V. N., Vener, A. V., and Ivanov, A. H. (1990) *Eur. J. Biochem. 194*, 879−887.
8. Gonzalez, M. A., Webb, M. R., Welsh, K. M., and Cooperman, B. S. (1984) *Biochemistry 23*, 797−801.
9. Janson, C. A., Degani, C., and Boyer, P. D. (1979) *J. Biol. Chem. 254*, 3743−3749.
10. Hewitt, E. J., and Nichols, D. J. (1963) in *Metabolic Inhibitors* (Hochster, R. M., and Quastel, J. H., Eds.) pp 311−436, Academic Press, New York.
11. Smith, F. A. (1970) *Handbook of Experimental Pharmacology*, Vol. 2, Parts 1 and 2, Springer-Verlag, New York.
12. Pinkse, M. W. H., Merkx, M., and Averill, B. A. (1999) *Biochemistry 38*, 9926−9936.
13. Smirnova, I. N., and Baykov, A. A. (1983) *Biokhimiya 48*, 1643−1653.
14. Baykov, A. A., Alexandrov, A. P., and Smirnova, I. N. (1992) *Arch. Biochem. Biophys. 294*, 238−243.
15. Avaeva, S. M., Velichko, T. I., Vorobyeva, N. N., Kurilova, S. A., Nazarova, T. I., and Sklyankina, V. A. (1999) *Biochemistry (Moscow) 64*, 169−174.
16. Morrisson, J. F., and Walsh, C. T. (1988) *Adv. Enzymol. Relat. Areas Mol. Biol. 61*, 201−301.
17. Baykov, A. A., Bakuleva, N. P., Nazarova, T. I., and Avaeva, S. M. (1977) *Biochim. Biophys. Acta 481*, 184−194.
18. Baykov, A. A., Tam-Villoslado, J. J., and Avaeva, S. M. (1979) *Biochim. Biophys. Acta 569*, 228−238.
19. Kurilova, S. A., Bogdanova, A. V., Nazarova, T. I., and Avaeva, S. M. (1984) *Bioorg. Khim. 10*, 1153−1160.
20. Avaeva, S., Ignatov, P., Kurilova, S., Nazarova, T., Rodina, E., Vorobyeva, N., Oganessyan, V., and Harutyunyan, E. (1996) *FEBS Lett. 399*, 99−102.
21. Heikinheimo, P., Pohjanjoki, P., Helminen, A., Tasanen, M., Cooperman, B. S., Goldman, A., Baykov, A., and Lahti R. (1996) *Eur. J. Biochem. 239*, 138−143.
22. Kolakowski, L. F., Jr., Schloesser, M., and Cooperman, B. S. (1988) *Nucleic Acids Res. 16*, 10441−10452.
23. Bradford, M. M. (1976) *Anal. Biochem. 72*, 248−254.
24. Salminen, T., Käpylä, J., Heikinheimo, P., Kankare, J., Goldman, A., Heinonen, J., Baykov, A. A., Cooperman, B. S., and Lahti, R. (1995) *Biochemistry 34*, 782−791.
25. Wong, S. C. K., Hall, D. C., and Josse, J. (1970) *J. Biol. Chem. 245*, 4335−4345.
26. Baykov, A. A., and Avaeva, S. M. (1981) *Anal. Biochem. 116*, 1−4.
27. Nýren, P., and Lundin, A. (1985) *Anal. Biochem. 151*, 504−509.
28. Fabrichniy, I. P., Kasho, V. N., Hyytiä, T., Salminen, T., Halonen, P., Dudarenkov, V. Yu., Heikinheimo, P., Chernyak, V. Ya., Goldman, A., Lahti, R., Cooperman, B. S., and Baykov, A. A. (1997) *Biochemistry 36*, 7746−7753.
29. Aziz, A., and Lyle, S. (1969) *Anal. Chim. Acta 47*, 49−56.
30. Kohlrausch, F. (1908) *Z. Phys. Chem. 64*, 129−169.
31. Baykov, A. A., Artjukov, A. A., and Avaeva, S. M. (1976) *Biochim. Biophys. Acta 429*, 982−992.
32. Springs, B., Welsh, K. M., and Cooperman, B. S. (1981) *Biochemistry 20*, 6384−6391.
33. Baykov, A. A., and Shestakov, A. S. (1992) *Eur. J. Biochem. 206*, 463−470.
34. Kasho, V. N., and Baykov, A. A. (1989) *Biochem. Biophys. Res. Commun. 161*, 475−480.
35. Hackney, D. D. (1980) *J. Biol. Chem. 255*, 5320−5328.
36. Huang, C. Y. (1979) *Methods Enzymol. 63*, 54−84.
37. Cleland, W. W. (1975) *Biochemistry 14*, 3220−3224.
38. Fersht, A. (1999) *Structure and Mechanism in Protein Science*, pp 125−127, 164−165, W. H. Freeman and Company, New York.


BI000627U